



Seismic activity of the Nevados de Chillán volcanic complex after the 2010 Mw8.8 Maule, Chile, earthquake



Cristian Farías^{a,*}, Matteo Lupi^{a,b}, Florian Fuchs^a, Stephen A. Miller^{a,c}

^a Steinmann Institute Geophysics/Geodynamics, University of Bonn, Bonn, Germany

^b Geological Institute, ETH, Zürich, Switzerland

^c The Centre for Hydrogeology and Geothermics, University of Neuchatel, Neuchatel, Switzerland

ARTICLE INFO

Article history:

Received 30 August 2013

Accepted 24 June 2014

Available online 9 July 2014

Keywords:

Volcano
Seismicity
Earthquakes
Chile
Maule
Aftershocks

ABSTRACT

Couplings between large magnitude subduction zone earthquakes and the subsequent response of their respective volcanic arcs are generally accepted, but the mechanisms driving this coupling are not known. The 2010 Maule earthquake (Mw8.8) ruptured approximately 500 km along strike in the south-central part of Chile, and provides an opportunity to investigate earthquake–volcano interactions. In an exploratory campaign, we deployed four broadband seismometers atop and surrounding the Nevados de Chillán volcanic complex because it is located directly behind one of the two primary slip patches of the Maule Earthquake. The data recorded (from December 2011 to April 2012) shows significant seismic activity, characterized by numerous volcano tectonic events and tremor episodes occurring within the volcanic complex. We recorded two strong aftershocks of the Maule earthquake (Mw 6.1 in January 2012, and Mw 7.1 in April 2012) and investigated the response of the volcano to the incoming seismic energy. We find that volcanic tremor increased significantly upon arrival of the seismic waves from the Mw 6.1 event, which was then followed a few hours later by a significant increase in volcano-tectonic events when tremors subsided. This delay between tremor and volcano-tectonic events suggests that fluid and/or magma migration (manifested as tremor) readjusted the local stress state that then induced the volcano-tectonic events. The increased activity persisted during the subsequent two weeks. In contrast, the Mw 7.1 event, which occurred at a similar epicentral distance from the volcano, did not produce any significant seismic response of the volcanic complex. Analysis of the particle velocity records of the two events shows that the volcanic system was perturbed in different ways because of the incidence angle of the incoming energy, inducing a back-elliptical vertical and fault parallel motion for the Mw 6.1 and no clear directional dependence for the Mw 7.1. This suggests dilatation-induced fluid migration within the complex, and a kinematic mechanism of the perturbation rather than the perturbation amplitude. Our results demonstrate the importance for continued monitoring of the arc behind Maule, with an increased seismometer and GPS array density to determine the style of deformation currently occurring in the arc.

© 2014 Elsevier B.V. All rights reserved.

1. Introduction

The influence of large magnitude earthquakes on volcanic activity has been a long-standing topic in Earth sciences. Recent improvements of monitoring networks combined with accurate analyses of historical records may allow a better understanding of the mechanisms underlying earthquake–volcano interactions. Static and dynamic stress triggering have been proposed to explain why volcanic systems may react to remote earthquakes. However, the debate on the physical processes controlling such interaction is still on-going and large data sets are necessary to distinguish between existing ideas (Marzocchi et al., 2002; Eggert and Walter, 2009; Bebbington and Marzocchi, 2011).

Static and dynamic stress triggering operate at different time-scales and distances. Dynamic triggering is induced by immediate effects caused by the passage of seismic waves through a geological system at or near a critical state (Hill et al., 2002; Ichihara and Brodsky, 2006). Numerical studies suggest that the convex structure of folded and faulted geological layers in volcanic and hydrothermal systems can focus seismic energy enhancing local stress variations (Davis et al., 2000; Lupi et al., 2013). This affects the physical equilibrium of the system and promotes fluid pressure variations by suggested mechanisms of rectified diffusion (Brodsky et al., 1998), volatile exsolution (Sparks et al., 1977; Manga and Brodsky, 2006), and other manifestations of rising fluids (Hill et al., 2002). Dynamic stress triggering operates over short time-scales (i.e. the immediate response to passing seismic waves), however, volcanic responses can occur up to several days after the earthquake because of the time required by the perturbed system to evolve. Brodsky and Prejean, (2005) and Hill (2008) show that dynamic stresses can

* Corresponding author. Tel.: +49 228 7360629.
E-mail address: cfarias@geo.uni-bonn.de (C. Farías).

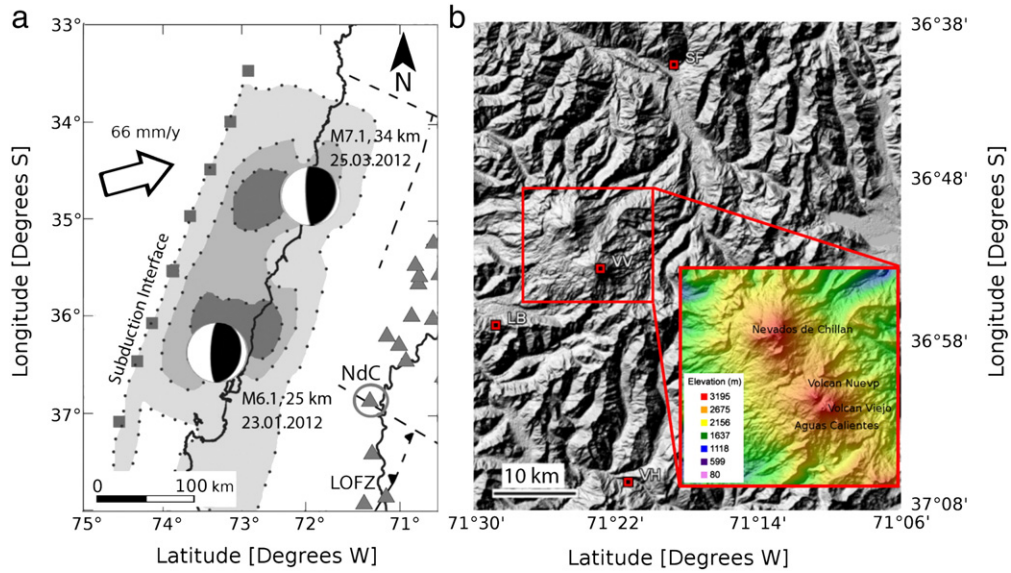


Fig. 1. a) Geodynamic setting of Chile between 33° and 38° and array distribution. The slip of the Maule earthquake is taken from USGS and dark gray indicates the maximum slip of 14 m which occurred at 35 km deep (Moreno et al., 2010). The southern and northern beach-balls mark the locations and focal mechanisms of the January 23rd, 2012, M6.1 and March 25th, 2012, M7.1 aftershocks, respectively. The northern portion of the Liquiñe–Ofqui fault zone (LOFZ) is also marked in the map. b) Topographic image of Nevados de Chillán volcanic complex. The red dotted squares indicate the location of the temporary stations and the inset shows the three main cones of the system.

travel great distances as stress decays according to $1/R^{1.66}$, with R being the distance from the hypocenter. Heat flux variations (Harris and McNutt, 2007; Delle Donne et al., 2010), seismic swarms (Hill et al., 1995) and transient deformation Johnston et al., 1995 are among the most common effects induced by transient seismic waves in volcanic centers. Examples of volcanic activity triggered by dynamic stress fronts are the eruption of Cordón Caulle volcano, Chile, 38 h after the Mw9.5 Valdivia (1960) earthquake (Lara et al., 2004), swarming in the Long Valley Caldera, USA, few minutes after the Mw7.3 Landers (1992)

Table 1

Historic eruptions of NdC volcano and historic mega-thrust earthquakes that occurred within 500 km from the complex, since 1900 AD. Distance stands for the distance between the epicenter location and the NdC. the eruptive events always occurred at the Volcán Nuevo, except once (2nd of July 1935, Volcán Viejo). For several historical records both the exact date and the VEI of the eruption are not specified. Mega-thrust events are shaded in gray and under “eruptive characteristics” we list historic information about the eruptions: C stands for central emission, FV for flank vent emission, RF for radial fissure emission, E for explosive eruption, PF for pyroclastic flows, PH for phreatic eruption, LF for lava flow, D for dome creation, and MF for mud flow. Historic eruptions and mega-thrust events are taken from Siebert et al., (2012) and SSN (2013), respectively.

Date	Magnitude	Epicenter	Eruptive characteristics	Eruption VEI	Distance [km]
16.08.1906	8.2	Valparaíso	FV, E, LF, MF	2	420
–,–,1907	–	–	FV, E	1	–
29.01.1914	8.2	Constitución	E	2	250
–,–,1923	–	–	FV	2?	–
10.04.1927	–	–	E	2?	–
30.11.1928	8.2	Talca	FV, E	2?	210
17.01.1934	–	–	E	2?	–
02.07.1935	–	–	FV, LF, MF	2?	–
24.01.1939	8.2	Chillán	–	–	100
–,–,1945	–	–	–	–	–
–,–,1946	–	–	FV, E	2?	–
22.05.1960	9.5	Valdivia	–	–	350
–,–,1965	–	–	FV	–	–
–,–,1972	–	–	FV	–	–
–07.1973	–	–	FV, E, PF, LF, D	2	–
03.03.1985	8.0	San Antonio	–	–	400
29.08.2003	–	–	C, RF, E, PH	1	–
21.01.2009	–	–	–	–	–
27.02.2010	8.8	Maule region	–	–	140

earthquake (Hill et al., 1993), the increase of seismicity of the Uturuncu volcano, Bolivia, immediately after the arrival of the surface waves induced by the Mw8.8 Maule earthquake (Jay et al., 2011), and the sudden increase in volcano-tectonic (VT) seismic activity at Llama volcano, Chile, after the Maule earthquake (Mora-Stock et al., 2012).

Static stress triggering mechanisms are proposed to explain marked increases of volcanic activity over longer time-scales (from months to decades). Static stress variations promoted by large magnitude earthquakes decay according to $1/R^3$ and are proposed to be caused by the post-seismic viscoelastic relaxation of the upper lithosphere (Walter and Amelung, 2007), or intermediate timescale changes in local kinematics (Lupi and Miller, 2014). Additionally, upwelling of deep fluids following mega-thrust earthquakes may be favored due to reduced normal stresses exerted on the volcanic plumbing system and that may modify the physical state of magmatic reservoirs. A new mechanism (Lupi and Miller, 2014) to explain the post-seismic increase of eruptive rates proposes that reductions of the horizontal principle stress ($\sigma_1 = \sigma_H$) induced by mega-thrust earthquake transforms the stress regime from a compressional environment to a strike slip faulting regime in the arc, which in turn favors the mobilization of magmas. This is in agreement with recent findings that show the coexistence of compressional and transpressional tectonic regimes over long time-scales in the Suban basin, Sumatra (Hennings et al., 2012), and with seismic activity occurring in volcanic arcs residing atop subduction zones recently affected by mega-thrust earthquakes (i.e. Sumatra, Chile, and Japan). The Mw9.5 Valdivia (1960) earthquake and its fore- and after-shocks (four foreshocks greater than Mw7.0, including a Mw7.9) induced large static stress variations in the volcanic arc. The geomechanical perturbation of this megathrust event may have induced the eruptions of Cordón Caulle and Copahue in 1960, Nevados de Chillán in 1965, and possibly Quizapu and Planchón Peteroa volcanoes in 1967. Static stress variations may last for decades as shown by cGPS measurements that indicate that the back-arc facing the 1960 Valdivia rupture zone is currently dominated by westwards displacements (Khazaradze et al., 2002; Brooks et al., 2011).

Central Chile is an ideal natural laboratory for investigating subduction zone earthquakes and the subsequent response of volcanic

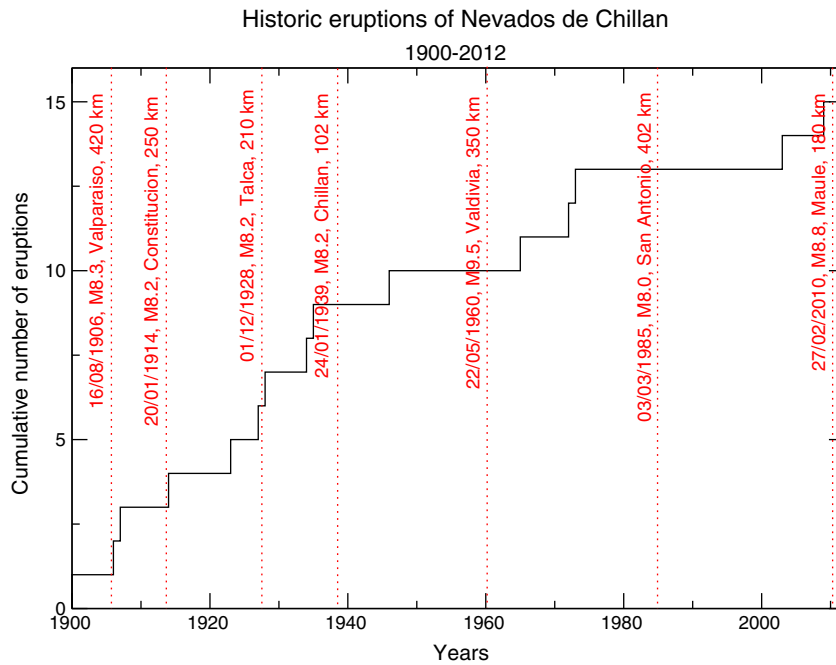


Fig. 2. Cumulative number of eruptions of Nevados de Chillán volcanic complex and mega-thrust events since 1900. Dotted vertical lines indicate mega-thrust earthquakes whose hypocenter was located less than 500 km from the volcano. Details on date, magnitude, and epicenter–volcano distance are shown in the vertical sentences. More information about eruptive behaviors can be found in Table 1. Note that the historic earthquake records may be affected by non systematic reporting.

arc because of the 2010 Mw 8.8 Maule earthquake and its rich aftershock sequence (including events as large as Mw 7.1). The area is extremely remote and rugged, and thus complicates the logistics of instrumentation, but this also offers a low-noise environment for seismic studies. It was observed in September 2010 that a Mw 5.2 earthquake at Planchón–Peteroa volcano was followed few hours later by a volcanic eruption, and our goal was to search for a similar behavior around the Nevados de Chillán volcano. We chose the Nevados de Chillán complex because it resides directly behind the high slip patch of the Maule earthquake, and has a geometrically intriguing feature of striking NW–SE that may be in part controlled by post-megathrust kinematics. In an exploratory campaign, we deployed four broadband stations from December 2011 to April 2012 around the Nevados de Chillán volcano, and recorded numerous volcano tectonic (VT) events, volcanic tremor, and background activity. We also recorded the response of the complex to two distant Maule aftershocks (Mw 6.1 at 192 km distance and Mw 7.1 at 200 km distance), and found different reactions of the volcano complex. The observed behavior provides insights into the mechanisms driving the triggered response of the volcano plumbing system.

Table 2

1. D velocity model used for NdC, with v_p and v_s being P-wave and S-wave velocities, respectively. This model is based on the work of Bohm et al. (2002) and it is currently in use by the Volcanologic Observatory of the Southern Andes (OVDAS, in Spanish) in Chile.

Depth [km]	v_p [km/s]	v_p/v_s
0	5.51	1.75
5	6.28	1.75
20	6.89	1.75
35	7.40	1.75
45	7.76	1.75
55	7.94	1.75
90	8.34	1.75

2. Geodynamic and geological setting of Central Chile

The tectonic setting of Chile from 33°S to 47°S is characterized by the oblique subduction of the Nazca plate underneath the South American plate (Fig. 1a).

Plate convergence of approximately 66 mm yr^{-1} , is accommodated by large-magnitude earthquakes along the length of the collision zone, and arc volcanism is ubiquitous. The most prominent geological feature of this part of Chile is the NNE–SSW striking Liquiñe–Ofqui fault, a right-lateral transpressional fault zone running from 38°S to 47°S. Monogenetic cones and basaltic to andesitic volcanoes (i.e. Villarrica, Llaima and Osorno) reside upon the Liquiñe–Ofqui fault, while more evolved volcanic systems (i.e. Nevados de Chillán and Copahue) reside along NW–SE striking lineaments, antithetic to the direction of the arc (Cembrano, 1992, 1996; Lavenu and Cembrano, 1999; Cembrano et al., 2000; Lange et al., 2008; Cembrano and Lara, 2009). Morphological evidence shows that the Liquiñe–Ofqui fault terminates approximately near the Copahue volcano (38°S) (Cembrano and Lara, 2009), but strike-slip moment tensor solutions of shallow seismic activity following the Maule earthquake document that strain partitioning extends in the arc also between 33°S and 38°S (Lupi and Miller, 2014). Nakamura (1977) suggests that the large scale distribution of volcanoes and their elongation can provide insights into the stress orientation at the regional scale. Lupi and Miller (2014) propose a ‘bookshelf’ mechanism to explain the occurrence of NW–SE trending lineaments across the Chilean and Argentinean border.

Table 3

Location of the four seismic stations deployed around Nevados de Chillán volcanic complex.

Location	Station	Latitude	Longitude	Elevation [m]
Las Bravas	LB	36.926 S	71.501 W	1799
Valle Hermoso	VH	37.078 S	71.340 W	1217
San Fabián	SF	36.670 S	71.287 W	824
Volcán Viejo	VV	36.872 S	71.370 W	3118

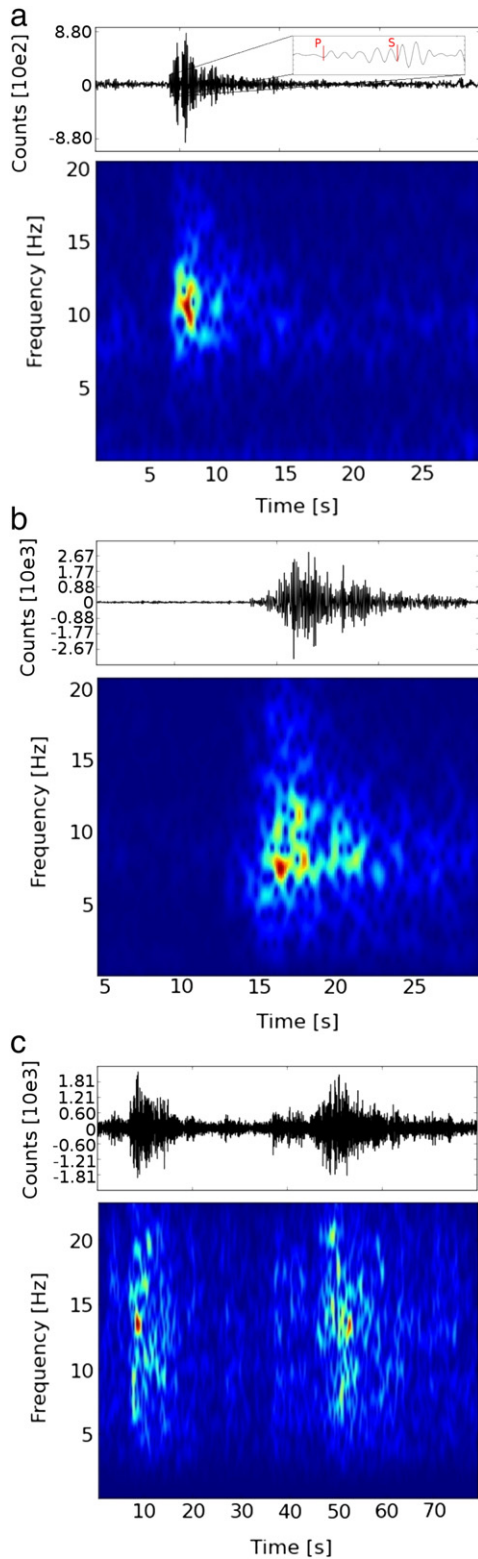


Fig. 3. Volcano tectonic events at the Nevados de Chillán. a) Deep VT, with an inlet with P- and S-wave arrivals marked in red, b) shallow VT, and c) high frequency swarm events found in the dataset for Nevados de Chillán from December 26th, 2011, to February 5th, 2012.

Nevados de Chillán experienced significant static stress changes induced by the Maule earthquake (Lupi and Miller, 2014), which was one reason for choosing this site for investigation. Additionally, Dziurma and Wehrmann (2010) studied the (pre-Maule) probability of a $VEI \geq 2$

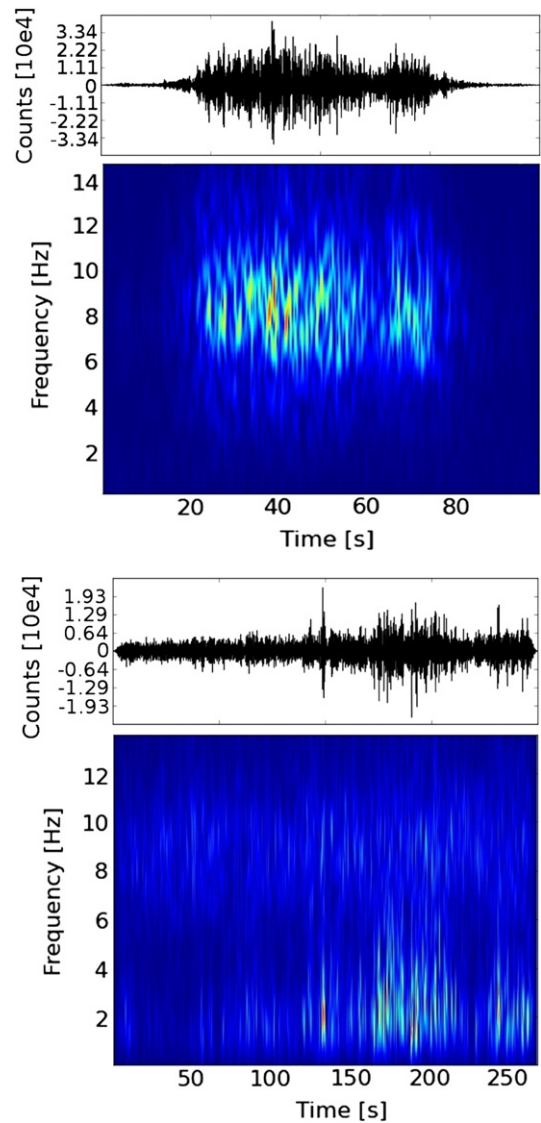


Fig. 4. Trace and spectrogram of tremor events. a) High frequency tremor event found throughout the normal activity of the volcano. b) Spasmodic volcanic tremor found in NdC complex after the swarm occurring on the 5th of January 2012.

eruption within the next ten years for ten Chilean volcanoes located between 33°S and 42°S . Their analyses showed that Llaima, Villarrica, and Nevados de Chillán volcanoes are the most likely candidates to erupt, followed by Puyehue and Calbuco volcanoes. From hereafter we will refer to the Nevados de Chillán volcanic complex as NdC.

The NdC volcanic complex (Fig. 1b) consists of 24 cones distributed along a 12 km long lineament striking approximately N290 (Fig. 1b) (Gonzalez-Ferrán, 1995). Volcán Nuevo, Volcán Viejo and Volcán Nevados are the three main volcanic centers. Volcán Nuevo resulted from the 1906 eruption that occurred immediately after the 1906 Valparaíso earthquake. Table 1 provides detailed information about the location of mega-thrust epicenters and the occurrence of volcanic activity at NdC. Due to the recent explosive activity of the Volcán Nuevo and to the rapid development of tourism in the area, the NdC is considered a high-risk volcano.

Fig. 2 shows the cumulative number of eruptions of the NdC during the past century and the occurrence of mega-thrust earthquakes nearby the NdC. Since the recorded VEI of many eruptions is similar, as showed in Table 1 the comparison of both time series can show interesting insights. It emerges that from 1900 to 1940 the volcano appeared more sensitive to external perturbations than in present the time, and only in three cases (1906, 1914, and 1928) the volcano entered in an eruptive

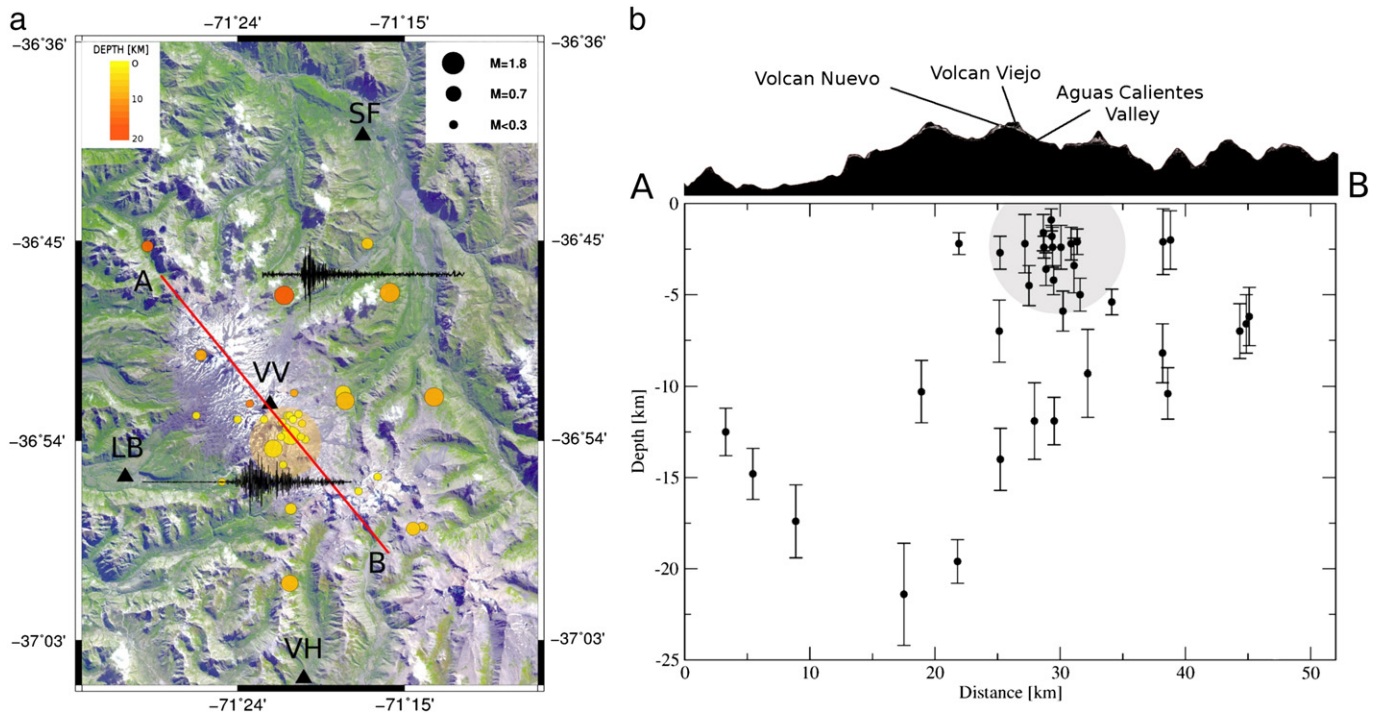


Fig. 5. a) Epicenter map of the seismic events within the Nevados de Chillán volcanic complex. Stations are marked as black triangles. Typical signals for shallow and deep VT events are drawn next to the location of the respective type of event. Note the difference of the waveform for both deep and shallow events. The orange circle marks the region where the non-locatable shallow events may be located. b) Locations of the events, from the perspective of the transverse cut marked by the red line in a), with A and B being the same points marked there. The error bars indicate the uncertainty of the locations in the vertical direction. Due to the geometry of the array, some extra uncertainty should be added in the left-right component of the locations in the cross section. The gray area is the projection along the line and the vertical direction of the yellow circle in a). Notice how most of the shallower events are located beneath the Aguas Calientes valley.

phase almost immediately after the occurrence of a mega-thrust earthquake.

3. Seismic network and methods

We deployed four Trillium 240 broadband seismometers equipped with Reftex130 data loggers around and atop the NdC complex from December 2011 to April 2012. Data were continuously recorded at a sampling rate of 100 Hz. We used a STA/LTA triggering algorithm (Withers et al., 1998) to mark the events, which we inspected manually to determine P- and S-wave arrivals. We used SEISAN (Ottmøller et al., 2011) and the 1D velocity model reported in Table 2. Our temporary network consisted of one station (VV) atop the NdC volcano surrounded by three stations (LB, VH, and SF) (Fig. 1) approximately 20 km from VV station (Table 3). Sporadic technical problems resulted in some discontinuity in

our dataset. The time window presented here (from December 26th, 2011 to February 5th, 2012) is continuous. Our array is the first ever to be used to study the NdC complex, but accessibility in this remote region resulted in a non-optimal geometry. Nevertheless, epicenter locations are well constrained north-south, but accuracy is limited in the east-west direction.

4. Results

We registered many different events during our experiment, with the vast majority recorded by station VV only and identified as volcano-tectonic (VT) earthquakes (McNutt, 2005; Wassermann, 2012), (Fig. 3), and tremor events (Fig. 4). In the first case, waveforms were 10 to 40 s long, with frequency content higher than 5 Hz. Among this type of event we defined three sub-categories: i) Events

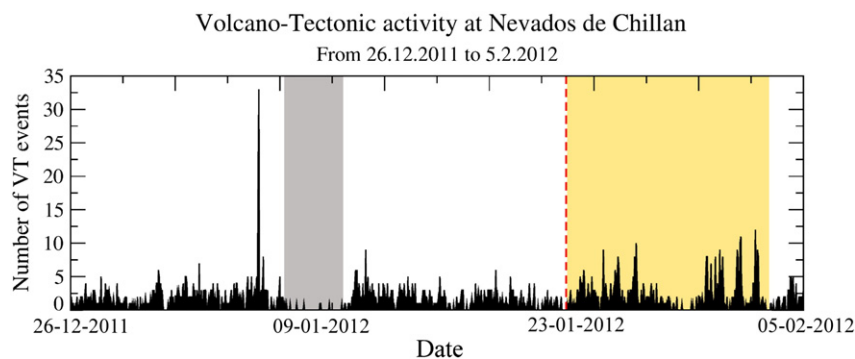


Fig. 6. Seismicity at Nevados de Chillán from December 26th, 2011, to February 5th, 2012. Gray and orange bands show periods of strong background tremor and triggered seismicity after a M6.1 regional earthquake, respectively.

Comparison between VT and tremor responses

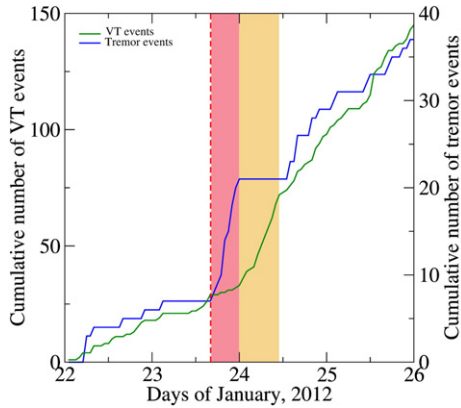


Fig. 7. Number of VT events per hour on Nevados de Chillán volcano before and after the M6.1 aftershock. The vertical dashed line marks the occurrence of the M6.1 and the red-shaded region highlights a strong increase of tremor events after the M6.1 earthquake. Next, tremor subsides and the number of VT events strongly increase (yellow-shaded area).

characterized by clear P- and S-wave onsets, with a dominant band around 8 Hz. Our network allowed us to manually locate approximately 50 earthquakes, with magnitudes ranging from MI 0.1 to MI 1.8 and depths from 0.1 km to 30 km; ii) events lacking of a clear S-wave onset, with a lower frequency band, typically around 6 Hz, which are shallow VT events according to the literature (Wassermann, 2012); iii) swarm events dominated by frequencies from 13 to 15 Hz (Fig. 3), which occurred between 16:00 UTC and 19:00 UTC of January 5th, 2012.

Tremor events last approximately 60 S and can also be separated into two sub-categories according to the shapes of the waveform and their occurrence patterns. The most common tremor was characterized by an excitement of the 8 Hz band, and was recorded by station VV only.

Similar events were recognized by Leet (1991) who described them as composite hydrothermal-magmatic tremor. Another possible source for this type of event is the superposition of several very shallow VT events. The second type of tremor occurred only between January 6th and January 8th, 20 h after the high frequency VT swarm (spike of Fig. 6). These signals were recorded by VV, LB, SF, and VH stations and were marked by clusters of high-amplitude signal dominated by 2 and 8 Hz frequencies (Fig. 4b).

4.1. Seismic activity

Fig. 5 shows the distribution of seismic events around the NdC. The NW–SE cross-section across the volcanic edifice shows that seismic activity clusters beneath the south-eastern flank of the cone Volcán Viejo, and more specifically below the Aguas Calientes valley, which is an area characterized by fumarolic activity and hot springs. We could not locate several VT events because they did not appear in all the stations of our array, and most of them were only registered by VV station. However, due to the lack of a clear S-wave onset in most of them, and the short time between the arrival of P and S-waves (generally separated by less than a second), it is likely that these events were originated at shallow depths, in the surrounding of Volcán Viejo cone (see shaded areas of Fig. 5). Deeper events are more dispersed and range from 10 to 25 km deep and fall outside the volcanic complex. Magnitudes of the shallow events range between MI 0.1 to MI 0.8 while the deeper events have somewhat larger magnitudes (the largest being a MI 1.8 earthquake).

Fig. 6 shows the number of VT events per hour recorded at station VV from December 26th, 2011, through February 5th, 2012. The peak on the left-hand side of the chart highlights a seismic swarm that occurred on January 5th, 2012 at 17:00 UTC, and lasted for 2.5 h. During this interval VT events are marked by a higher frequency content (see Fig. 3c), with a dominant band around 13–15 Hz, and with a remarkably shorter coda compared to other VT earthquakes recorded during our seismic campaign. Twenty hours after this swarm, the VT event rate decreased down to approximately one event per hour and continuous tremor marked by clusters of high-amplitudes emerged.

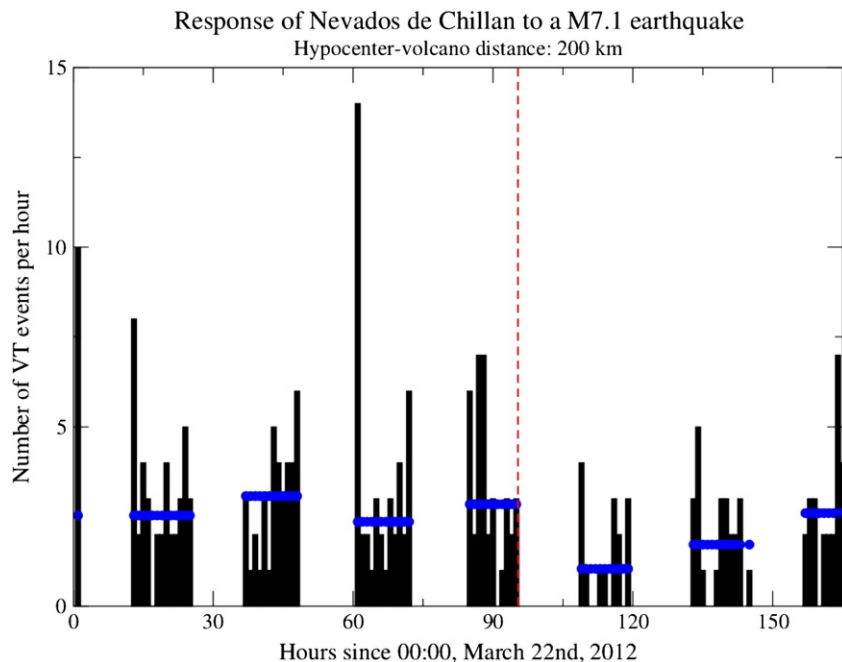


Fig. 8. Number of VT events per hour occurring at the Nevados de Chillán volcano before and after the M7.1 aftershock. The vertical dashed line marks the occurrence of the M6.1 and blue lines mark the average number of VT events per hour.

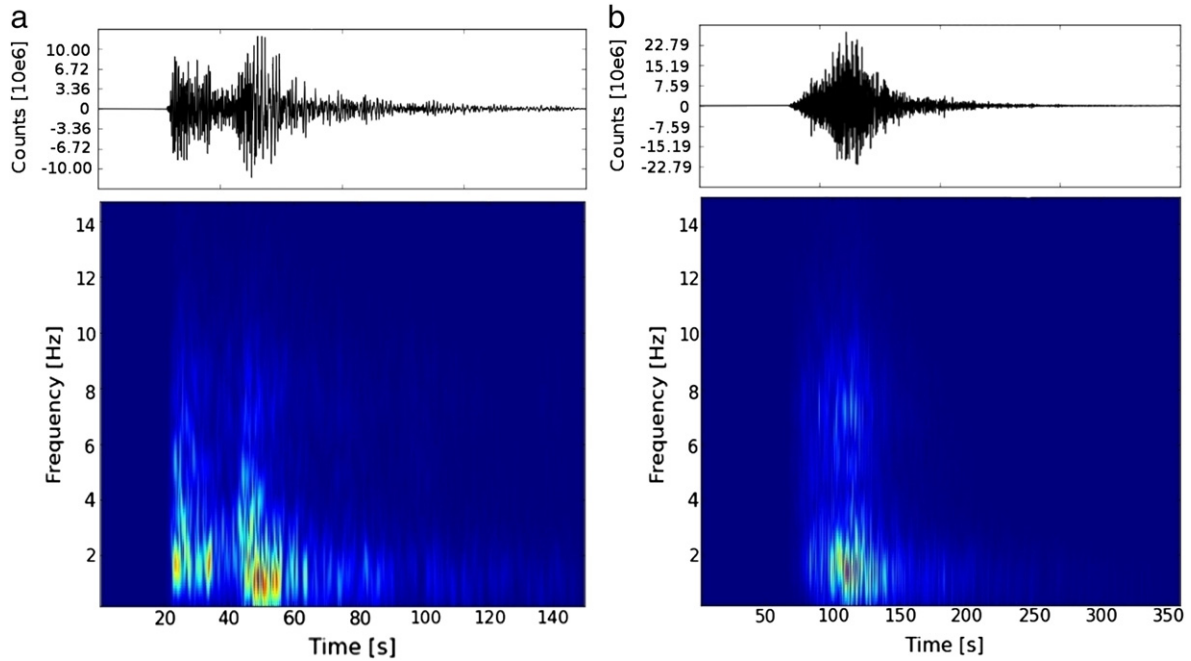


Fig. 9. Waveform and spectra for the M6.1 and M7.1 earthquakes.

4.2. Response to large regional earthquakes

On January 23rd, 2012, a Mw 6.1 aftershock occurred at the subduction interface (25 km deep, USGS), approximately 192 km from the NdC volcanic complex (Fig. 1). The volcanic activity at NdC before the event was low, with less than one event per hour. The Mw 6.1 earthquake occurred at 16:04 UTC, afterwards (17:04 UTC) tremor activity increased noticeably and lasted for approximately 9 h. When tremor stopped at 02:00 UTC, the VT event rate increased to an average of 3.5 events/h.

Fig. 7 shows the total number of tremor and VT events before and after the occurrence of the Mw 6.1 earthquake, highlighting the onset of double-couple events after tremor subsided. A second large aftershock of the Maule mega-thrust earthquake occurred on March 25th, 2012, 200 km away (34 km deep, USGS) from the NdC complex (Fig. 1). At the time, station VV was suffering 12 hours of daily data loss due to energy-storage issues. Nevertheless, we captured the signal of the Mw 7.1 earthquake and analyzed the VT rate of the available data. Comparing the Mw 7.1 post-seismic records with the ones that followed

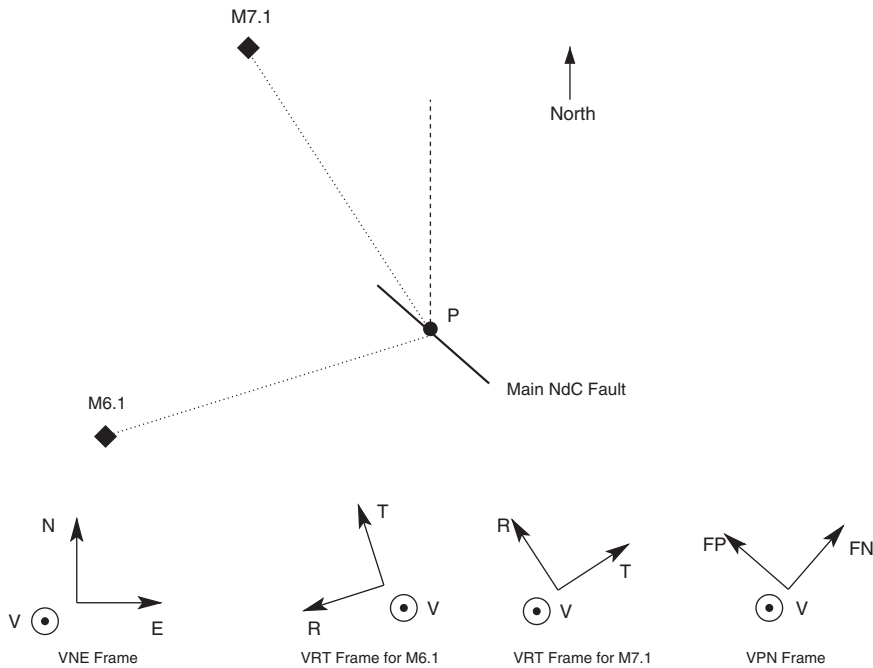


Fig. 10. Schematic representation of the relative location of the Mw6.1 and Mw7.1 events to the main lineament of the Nevados de Chillán volcanic complex, and the different coordinate frames used in our analysis. More detail on each one of the frames is given on the text.

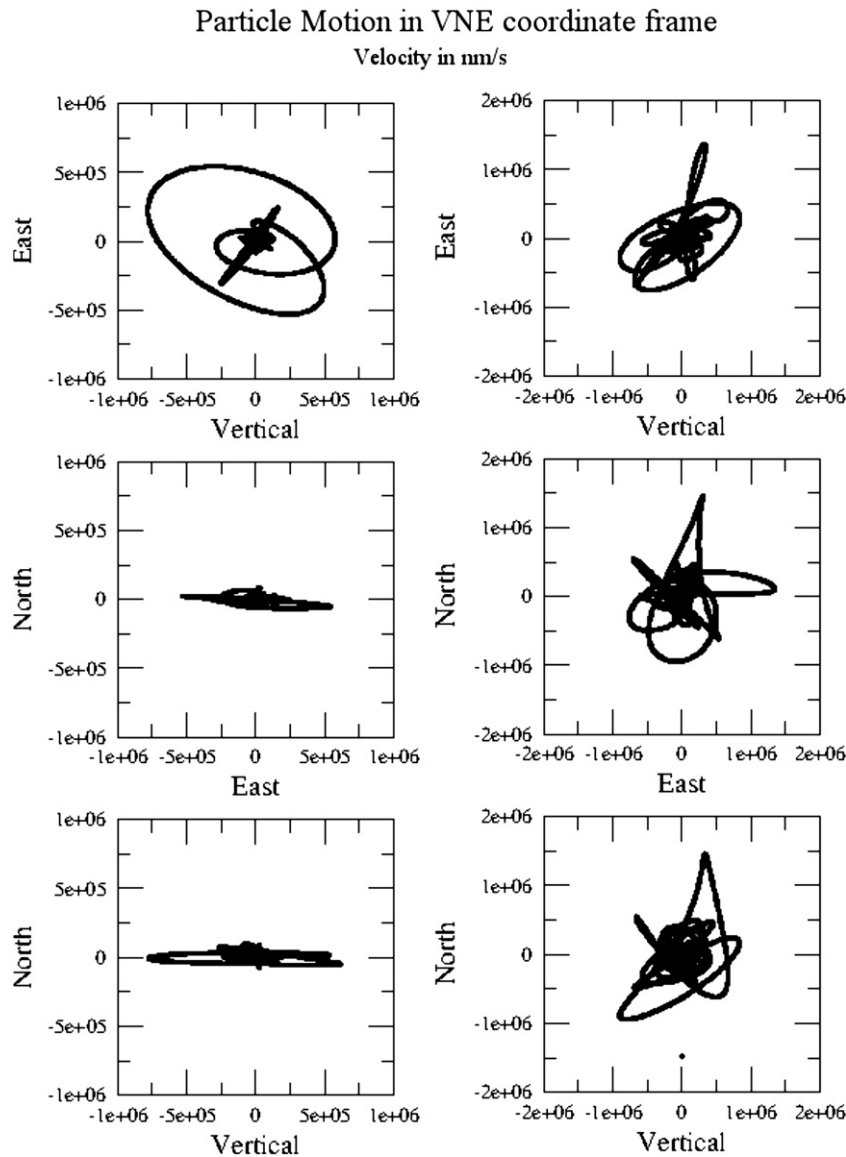


Fig. 11. Velocity particle motion plots in Volcan Viejo station for the Mw6.1 and Mw7.1 event in the VNE frame. The signal was filtered between 0.01 Hz and 0.1 Hz and the velocity is measured in mm/s. The N-V axes identify the north-vertical plane, E-V the east-vertical plane and the N-E axes identify the north-east plane. Note the dominant oscillatory behavior induced by the M6.1 earthquake on the N-Z and N-E planes in contrast to the motion induced by the M7.1.

the Mw 6.1 we found that before the Mw 7.1 earthquake the seismic activity was particularly intense with an average of three events per hour (Fig. 8). However, the available data show that the VT rate decreased to one event per hour after the earthquake. Although our analysis is biased by the lack of data, the reduction of the number of events per hour following the Mw 7.1 aftershock is clearly shown. This type of response is similar to that recorded for Mt. Wrangell and Mt. Veniaminof volcanoes after the 2002, Mw 7.9 Denali earthquake (Sanchez and McNutt, 2004).

5. Discussion

We investigated the seismic activity of the NdC complex after the Maule earthquake and found that seismic activity mainly occurs from 2 to 5 km deep beneath the region called Aguas Calientes, a valley known for its natural hot springs and fumaroles. Deeper events also occur below the volcanic complex down to approximately 20 km deep. We did not locate several low-magnitude seismic events because they did not appear on a sufficient number of stations. However, their

waveforms are characteristic of shallow VT events. This points to a local origin that may be within the volcanic system, possibly beneath the Aguas Calientes valley. The location of this shallow seismicity plus the type of tremor events we recorded in our campaign suggest that the activity at the NdC has a strong hydrothermal component, thus making the volcano an active hydrothermal-magmatic system.

We observed different responses of the NdC to two large Maule aftershocks (Mw 6.1, Fig. 7 and Mw 7.1, (Fig. 8) originating at similar hypocentral distances from the NdC. We identified a triggered response of the NdC after the Mw 6.1 event but not after the Mw 7.1 event. Note that although data loss during the Mw 7.1 event introduces a bias, we registered a decrease in VT when compared to the behavior prior to the Mw 7.1 event (blue lines in Fig. 8 indicate the average rate). Fig. 9 shows the waveforms and spectra of the two aftershocks of the Maule earthquake. The maximum amplitudes in a ground motion seismograph of the two events are comparable and are on the order of 1 to 2 mm for the vertical component at station VV. Using particle motion plots, we investigated the effect of the incidence angle of the incoming seismic waves and

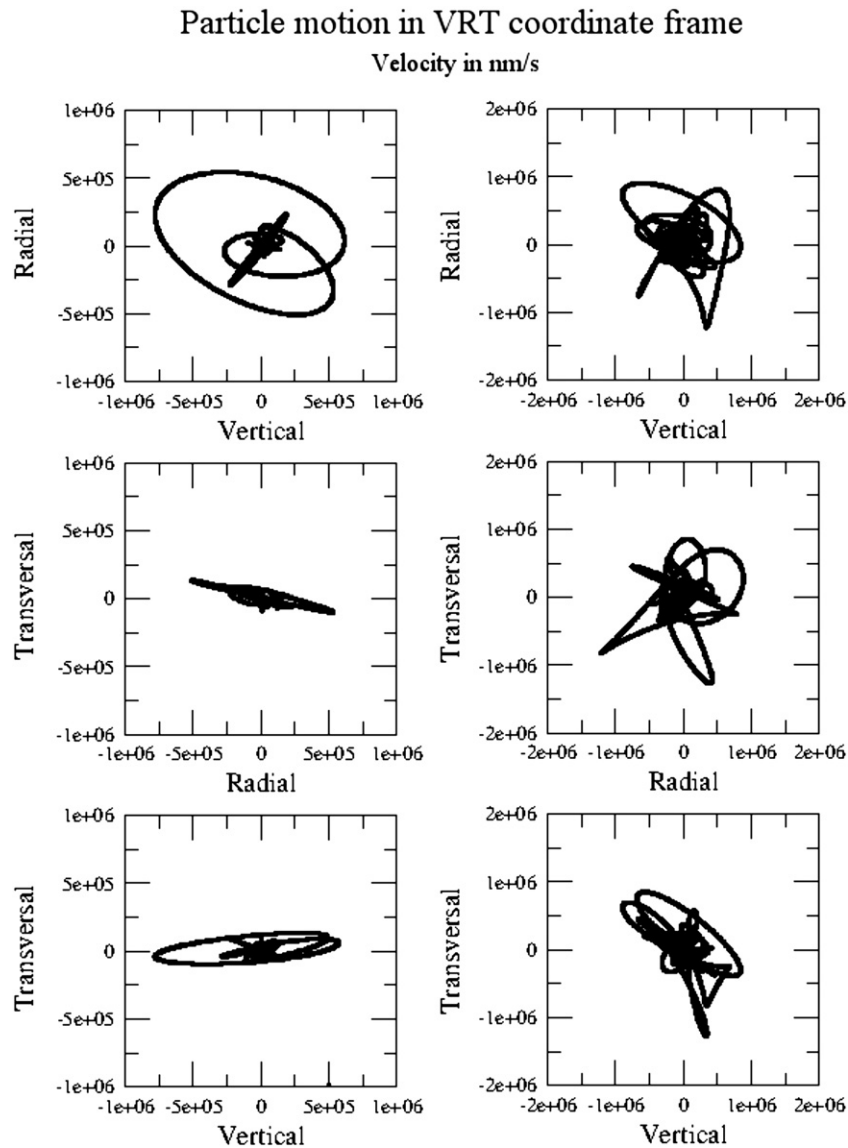


Fig. 12. Velocity particle motion plots in Volcan Viejo station for the Mw6.1 and Mw7.1 event, each one in a frame rotated to its backazimuth (VRT frame). The signal was filtered between 0.01 Hz and 0.1 Hz and the velocity is measured in nm/s. For each earthquake, the R-V axes identify the radial-vertical plane, T-Z the transverse-vertical plane and the T-R axes identify the transverse-radial plane.

found that the difference between the effect produced by the two events may lie there. Fig. 10 shows a scheme of the different coordinate frames used in the observation point given by the location of VV station. Figs. 11, 12, and 13 show particle velocity motion plots for both earthquakes in station VV, filtered between 0.01 Hz and 0.1 Hz, in different coordinate systems: vertical/north/east (VNE), vertical/radial/transversal (VRT) for both events, and vertical/NdC fault normal/NdC fault parallel (VNP). In the VNE frame the most noticeable feature is how the particle motion induced by the Mw6.1 event presents a dominant motion along the east and vertical directions, with amplitudes around 10 mm s^{-1} , while the Mw7.1 event induced velocities with maximum amplitudes on the order of 20 mm s^{-1} , but without any preferential orientation. The induced particle motion in the VRT frame shows how, for the Mw6.1 event, the transverse movement is significantly smaller than the radial one, suggesting that the wave train is mostly dominated by Rayleigh waves rather than Love waves. In the case of the Mw7.1 event, there is no clear dominance of either transverse or radial motion modes. Finally, on the VPP frame it can be appreciated how the

Mw6.1 event induced a motion oblique to the main fault of the NdC complex, which may help to create a fault-parallel motion, thus enhancing a stress change along the main lineament of the system. On the other hand, the Mw7.1 does not show a preferred direction of motion.

The analysis of particle motion in the three different coordinate frames suggests that the Mw6.1 event may have induced an elliptical motion in the main fault of the NdC, with dominant fault-parallel and vertical components, thus promoting the creation of spaces for the fluids to arise and move along the lineament, as reflected by the important increase on seismicity right after the passage of the wave train. This indicates that the observed behavior of triggered tremor followed by VT events was controlled by dilatational processes due to the Rayleigh waves. This is consistent with other studies that report triggered tremor due to the passage of the Rayleigh waves in regions like Japan after the 2004 Sumatra–Andean earthquake (Miyazawa and Mori, 2005, 2006). In a more general work frame, our observations are also consistent with other studies showing permeability increases correlating with passing seismic waves (Kitagawa et al., 2002; Elkhoury et al., 2006).

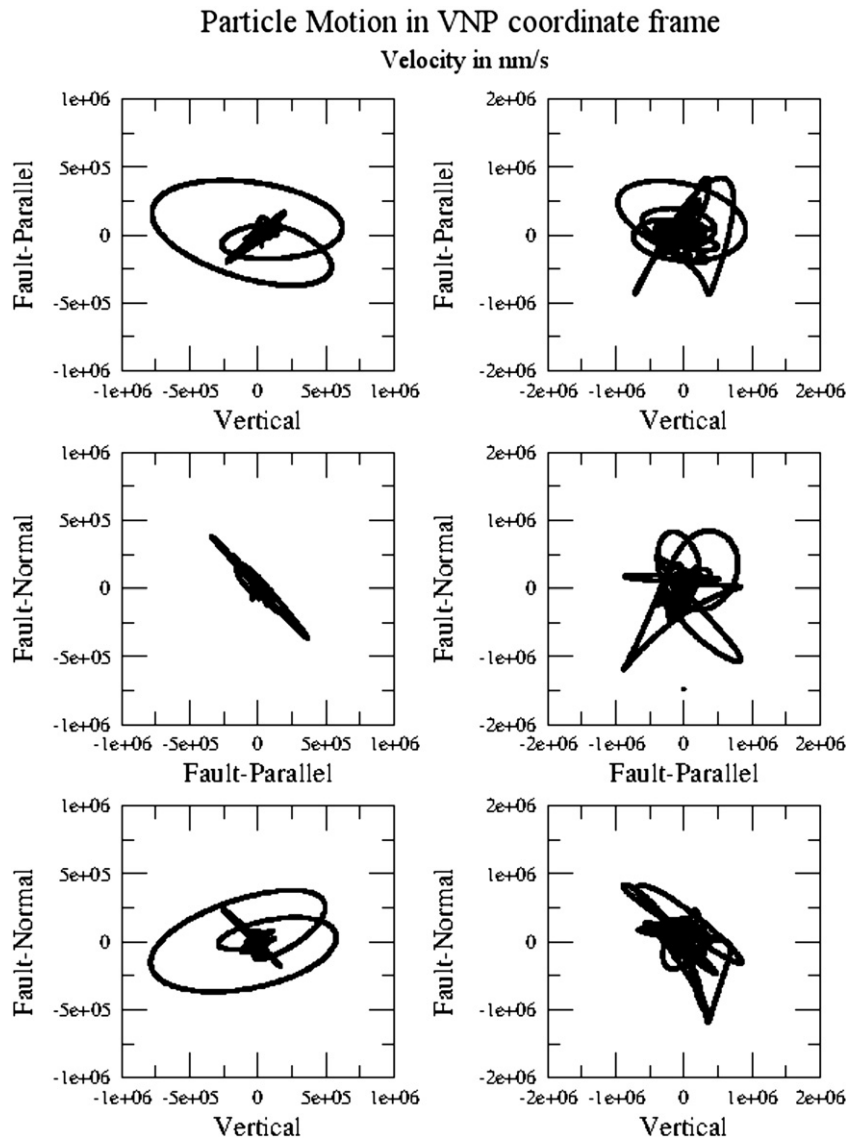


Fig. 13. Velocity particle motion plots in Volcan Viejo station for the Mw6.1 and Mw7.1 event, in the VNP coordinate frame. The signal was filtered between 0.01 Hz and 0.1 Hz and the velocity is measured in mm/s. The FP-Z axes identify the fault-parallel/vertical plane, FN-Z the fault-normal/vertical plane and the FP-FN axes identify the fault-parallel/fault-normal plane.

6. Conclusions

We presented data from a seismic campaign that took place from December 2011 to April 2012 around the Nevados de Chillán (NdC) volcanic complex, in Central-Southern Chile. We recorded numerous volcano-tectonic (VT) and tremor events within the volcanic complex. The majority of the events was shallower than 5 km deep and occurred beneath the south-east flank of the volcano. Two major aftershocks (Mw 6.1 and Mw 7.1) of the 2010 Maule earthquake, at similar distances for the NdC elicited different responses. The response to the Mw6.1 event was characterized by an increase of tremor activity 1 h after the earthquake, followed by a marked increase of VT events when the tremor subsided. This strongly suggests a fluid driven mechanism induced by the passage of the seismic waves. In contrast, the Mw 7.1 event did not trigger a response of NdC. We propose that this difference in behavior is a result of the incidence angle of incoming energy, where the Mw 6.1 showed predominantly EW (arc-oblique) particle motion and the Mw 7.1 showed no particular oscillatory path. An alternative explanation could be that the response to the Mw 6.1 event relaxed the system and therefore was not perturbed sufficiently to

induce a response from the Mw 7.1. Future seismic campaigns with a higher density array will allow triggered responses to be constrained with better accuracy.

The volcanic arc behind the Maule earthquake is an excellent natural laboratory for investigating earthquake–volcano interactions, and should be instrumented in the future to better understand earthquake–volcano interactions and the internal dynamics of perturbed arc systems.

Acknowledgments

Cristian Fariás thanks the Becas Chile Scholarship Program (72120406) for supporting his work. Humanitus Sidoarjo fund is thanked for supporting Matteo Lupi. Matteo Lupi was also partially supported by the ETH Zurich Postdoctoral fellowship. Daniel Basualto from Observatorio Volcanológico de los Andes del Sur (OVDAS) is acknowledged for providing us the 1-D velocity model. Cristian Sepulveda and Gustavo Aldea are acknowledged for their help in the field and logistical support.

References

- Bebbington, M., Marzocchi, W., 2011. Stochastic models for earthquake triggering of volcanic eruptions. *J. Geophys. Res.* B 116.
- Bohm, M., Lüth, S., Echlter, H., Asch, G., Bataille, K., Bruhn, C., Rietbrock, A., Wigger, P., 2002. The Southern Andes between 36 and 40°S latitude: seismicity and average seismic velocities. *Tectonophysics* 356, 275–289.
- Brodsky, E., Prejean, S., 2005. New constraints on mechanism of remotely triggered seismicity at Long Valley Caldera. *J. Geophys. Res.* B 110.
- Brodsky, E., Sturtevant, B., Kanamori, H., 1998. Earthquakes, volcanoes, and rectified diffusion. *J. Geophys. Res.* 103, 23827–23838.
- Brooks, B., Bevis, M., Whipple, K., Arrowsmith, J., Foster, J., Zapata, T., Kendrick, E., Minaya, E., Echalar, A., Blanco, M., Euillades, P., Sandoval, M., Smalley, R., 2011. Orogenic-wedge deformation and potential for great earthquakes in the central andean backarc. *Nat. Geosci.* 4, 380–383.
- Cembrano, J., 1992. The Liquiñe–Ofqui Fault Zone (LOFZ) in the Province of Palena: Field and Microstructural Evidence of a Ductile–Brittle Dextral Shear Zone. Universidad de Chile, Departamento de Geología, Comunicaciones.
- Cembrano, J., Lara, L., 2009. The link between volcanism and tectonics in the southern volcanic zone of the Chilean Andes: a review. *Tectonophysics* 471, 96–113.
- Cembrano, J., Hervé, F., Lavenu, A., 1996. The Liquiñe Ofqui fault zone: a long-lived intra-arc fault system in Southern Chile. *Tectonophysics* 259, 55–66.
- Cembrano, J., Schermer, E., Lavenu, A., Sanhueza, A., 2000. Contrasting nature of deformation along an intra-arc shear zone, the Liquiñe–Ofqui fault zone, Southern Chilean Andes. *Tectonophysics* 319, 129–149.
- Davis, P., Rubinstein, J., Liu, K., Gao, S., Knopoff, L., 2000. Northridge earthquake damage caused by geologic focusing of seismic waves. *Science* 289, 1746–1750.
- Delle Donne, d., Harris, A., Ripepe, M., Wright, R., 2010. Earthquake-induced thermal anomalies at active volcanoes. *Geology* 38, 771–774.
- Dzierma, Y., Wehrmann, H., 2010. Eruption time series statistically examined: probabilities of future eruptions at Villarrica and Llaima volcanoes, southern volcanic zone, Chile. *J. Volcanol. Geotherm. Res.* 193, 82–92.
- Eggert, S., Walter, T., 2009. Volcanic activity before and after large tectonic earthquakes: observations and statistical significance. *Tectonophysics* 471, 14–26.
- Elkhoury, J.E., Brodsky, E.E., Agnew, D.C., 2006. Seismic waves increase permeability. *Nature* 441, 1135–1138.
- Gonzalez-Ferrán, O., 1995. Volcanes de Chile. Instituto Geográfico Militar, Chile.
- Harris, R.N., McNutt, M.K., 2007. Heat flow on hot spot swells: evidence for fluid flow. *J. Geophys. Res.* B 112.
- Hennings, P., Allwardt, P., Paul, P., Zahm, C., Alley, H., Kirschner, R., Lee, B., Hough, E., 2012. Relationship between fractures, fault zones, stress, and reservoir productivity in the Suban gas field, Sumatra, Indonesia. *Am. Assoc. Pet. Geol. Bull.* 96, 753–772.
- Hill, D., 2008. Dynamic stresses, coulomb failure, and remote triggering. *Bull. Seism. Soc. Am.* 102, 2313–2336.
- Hill, D., Reasenber, A., Michael, A., Arabaz, W., Beroza, G., Brumbaugh, D., Brune, J., Castro, R., Davis, S., dePollo, D., Ellsworth, W., Gombert, J., Harmsen, S., House, L., Jackson, S., Johnston, J., Jones, L., Keller, R., Malone, S., Munguia, L., Nava, S., Pechmann, J., Sanford, A., Simpson, R., Smith, R., Stark, M., Stickney, M., Vidal, A., Walter, S., Wong, V., Zollweg, J., 1993. Seismicity remotely triggered by the magnitude 7.3 Landers, California, earthquake. *Science* 260, 1617–1623.
- Hill, D., Johnston, M., Langbein, J., Bilham, R., 1995. Response of Long Valley Caldera to the $m = 7.3$ Landers, California, earthquake. *Geophys. Res. Lett.* 100, 12985–13005.
- Hill, D., Pollitz, P., Newhall, C., 2002. Earthquake–volcano interactions. *Phys. Today* 55, 41–47.
- Ichihara, M., Brodsky, E., 2006. A limit on the effect of rectified diffusion in volcanic systems. *Geophys. Res. Lett.* 32.
- Jay, J., Pritchard, M., West, M., Christensen, D., Haney, M., Minaya, E., Sunagua, M., McNutt, S., Zabala, M., 2011. Shallow seismicity, triggered seismicity, and ambient noise tomography at the long-dormant Uturuncu Volcano, Bolivia. *Bull. Volcanol.* 74, 817–837.
- Johnston, M., Hill, D., Langbein, J., Bilham, R., 1995. Transient deformation during triggered seismicity from the 28 June 1992 $m_w = 7.3$ Landers earthquake at Long Valley Volcanic Caldera, California. *Bull. Seism. Soc. Am.* 85, 787–795.
- Khazaradze, G., Wang, K., Klotz, J., Hu, Y., He, J., 2002. Prolonged post-seismic deformation of the 1960 great Chile earthquake and implications for mantle rheology. *Geophys. Res. Lett.* 29, 2050.
- Kitagawa, Y., Fujimori, K., Koizumi, N., 2002. Temporal change in permeability of the rock estimated from repeated water injection experiments near the Nojima fault in Awaji Island, Japan. *Geophys. Res. Lett.* 29, 1483.
- Lange, D., Cembrano, J., Rietbrock, A., Haberland, C., Dahm, T., Bataille, K., 2008. First seismic record for intra-arc strike-slip tectonics along the Liquiñe–Ofqui fault zone at the obliquely convergent plate margin of the Southern Andes. *Tectonophysics* 455, 14–24.
- Lara, L., Naranjo, J., Moreno, H., 2004. Rhyodacitic fissure eruption in Southern Andes (Cordón Caulle; 40.5°S) after the 1960 (m_w : 9.5) Chilean earthquake: a structural interpretation. *J. Volcanol. Geotherm. Res.* 138, 127–138.
- Lavenu, A., Cembrano, J., 1999. Compressional and transpressional stress pattern for pliocene and quaternary brittle deformation in forearc and intra-arc zones (Andes of Central and Southern Chile). *J. Struct. Geol.* 21, 1669–1691.
- Leet, R., 1991. Investigation of Hydrothermal Boiling and Steam Quenching as Possible Sources of Volcanic Tremor and Geothermal Noise Ph.D. thesis University of Washington.
- Lupi, M., Miller, S., 2014. Short-lived tectonic switch mechanism for long-term pulses of volcanic activity after mega-thrust earthquakes. *Solid Earth* 5, 13–24.
- Lupi, M., Saenger, H., Fuchs, F., Miller, S., 2013. Lusi mud eruption triggered by geometric focusing of seismic waves. *Nat. Geosci.* <http://dx.doi.org/10.1038/ngeo1884>.
- Manga, M., Brodsky, E., 2006. Seismic triggering of eruptions in the far field: volcanoes and geysers. *Annu. Rev. Earth Planet. Sci.* 34, 263–291.
- Marzocchi, W., Casarotti, E., Piersanti, A., 2002. Modeling the stress variations induced by great earthquakes on the largest volcanic eruptions of the 20th century. *J. Geophys. Res.* 107.
- McNutt, S., 2005. Volcanic seismology. *Annu. Rev. Earth Planet. Sci.* 32, 461–491.
- Miyazawa, M., Mori, J., 2005. Detection of triggered deep low-frequency events from the 2003 Tokachi-oki earthquake. *Geophys. Res. Lett.* 32.
- Miyazawa, M., Mori, J., 2006. Evidence suggesting fluid flow beneath Japan due to periodic seismic triggering from the 2004 Sumatra–Andaman earthquake. *Geophys. Res. Lett.* 33.
- Mora-Stock, C., Thorwart, M., Wunderlich, T., Bredemeyer, S., Hansteen, T., Rabbel, W., 2012. Comparison of seismic activity for Llaima And Villarrica volcanoes prior to and after the Maule 2010 earthquake. *Int. J. Earth Sci.* 1–14.
- Moreno, M., Rosenau, M., Oncken, O., 2010. 2010 Maule earthquake slip correlates with pre-seismic locking of Andean subduction zone. *Nature* 467, 198–202.
- Nakamura, K., 1977. Volcanoes as possible indicators of tectonic stress orientation: principle and proposal. *J. Volcanol. Geotherm. Res.* 2, 1–16.
- Ottmøller, L., Voss, P., Havskov, J., 2011. Seisan Earthquake Analysis Software for Windows, Solaris, Linux, and MacOSx.
- Sanchez, J., McNutt, S., 2004. Intermediate-term declines in seismicity at Mt. Wrangell and Mt. Veniaminof volcanoes, Alaska, following the 3 November 2002 m_w 7.9 Denali fault earthquake. *Bull. Seism. Soc. Am.* 94.
- Siebert, L., Simkin, T., Kimberly, P., 2012. Volcanoes of the World. University of California Press, USA.
- Sparks, R., Sigurdsson, J., Wilson, L., 1977. Magma mixing: a mechanism for triggering acid explosive eruptions. *Nature* 267, 315–318.
- SSN, 2013. <http://www.sismologia.cl/links/terremotos/index.html> Technical Report. Chilean Seismological Service.
- Walter, T., Amelung, F., 2007. Volcanic eruptions following $m \geq 9$ megathrust earthquakes: implications for the Sumatra–Andaman volcanoes. *Geology* 35, 539–542.
- Wassermann, J., 2012. Volcano Seismology, IASPEI New Manual of Seismological Observatory Practice 2. Deutsches GeoForschungsZentrum GFZ, Potsdam.
- Withers, M., Aster, R., Young, C., Beiriger, J., Harris, M., Moore, S., Trujillo, J., 1998. A comparison of select trigger algorithm for automated global seismic phase and event detection. *Bull. Seism. Soc. Am.* 88, 95–106.